



Nearshore wave processes in the Iroise Sea: field measurements and modelling

Jean-François Filipot, Volker Roeber, Martial Boutet, Cédric Ody, Cyril Lathuiliere, Stéphanie Louazel, Thierry Schmitt, Fabrice Ardhuin, André Lusven, Michel Outré, et al.

► To cite this version:

Jean-François Filipot, Volker Roeber, Martial Boutet, Cédric Ody, Cyril Lathuiliere, et al.. Nearshore wave processes in the Iroise Sea: field measurements and modelling. Coastal Dynamics 2013 - 7th International Conference on Coastal Dynamics, Jun 2013, Arcachon, France. p. 605-614. hal-00879930

HAL Id: hal-00879930

<https://hal.science/hal-00879930>

Submitted on 11 Aug 2014

HAL is a multi-disciplinary open access archive for the deposit and dissemination of scientific research documents, whether they are published or not. The documents may come from teaching and research institutions in France or abroad, or from public or private research centers.

L'archive ouverte pluridisciplinaire **HAL**, est destinée au dépôt et à la diffusion de documents scientifiques de niveau recherche, publiés ou non, émanant des établissements d'enseignement et de recherche français ou étrangers, des laboratoires publics ou privés.

NEARSHORE WAVE PROCESSES IN THE IROISE SEA: FIELD MEASUREMENTS AND MODELLING

Jean-François Filipot¹, Volker Roeber², Martial Boutet¹, Cédric Ody¹, Cyril Lathuiliere¹, Stéphanie Louazel¹, Thierry Schmitt¹, Fabrice Ardhuin³, André Lusven¹, Michel Outré¹, Serge Suanez⁴,
Alain Hénaff⁴

Abstract

A sample of observations gathered during the PROTEVS-VAGUES 2012 field experiment is presented. A focus is done on the analysis of five instruments deployed over Sein Island south coast. Waves and their effects on the mean water level are examined in the case of a long wave event that occurred on February 11, 2013. The nonlinear wave processes observed in the nearshore are found to be similar to those found over tropical reefs. Preliminary simulations of the Boussinesq type model, BOSZ, show encouraging results. BOSZ captures the main hydrodynamic processes such as refraction, shoaling, and wave breaking, but also accounted for second-order processes such as wave setup and the inherent recirculation in the surf zone.

Keywords

Numerical modeling, flood hazards, coastal erosion, infra-gravity waves, Brittany.

1. Introduction

Coastal communities and ecosystems in low-lying areas are vulnerable to impacts resulting from storm surge or large swell events in combination with sea-level rise. Numerical modeling has become an indispensable tool for coastal engineering design and hazard assessment. However, suitable numerical models are hard to find. A research initiative between the French Naval Hydrographic and Oceanographic Service (SHOM) and the Department of Ocean and Resources Engineering at the University of Hawaii, has been focusing on the development and validation of numerical models for coastal engineering and disaster management to address future problems in coastal dynamics. Recently, the Department of Ocean and Resources Engineering at the University of Hawaii has completed a higher-order Boussinesq-type model for nearshore wave processes. The model has been validated with a series of laboratory benchmark data, field data, as well as hurricane scenarios in tropical and extra-tropical environments, particularly with wave scenarios generated by Hurricane Iniki, Kauai, Hawaii, and Hurricane Ivan, Gulf coast, Florida. In the mean time, SHOM is pursuing research on wave spectral models and on their extension toward beach processes. A field experiment was further conducted in the Iroise Sea during the winter 2012-2013 with the objective of collecting wave, current, and water level data from extreme oceanographic conditions. The corresponding observations compose an important database for model validation and understanding of the nearshore physical processes during extreme storm events.

A sample of this recent experiment is presented here and serves for preliminary model validation. The study focuses on the nonlinear wave transformation over the south coast of Sein Island.

¹ SHOM, Brest, FRANCE.

² University of Hawaii at Manoa, Honolulu, Hawaii, USA.

³ IFREMER, Laboratoire d'Océanographie Spatiale, Plouzané, FRANCE.

⁴ LETG-Géomer-Brest, IUEM, Plouzané, FRANCE.

2. Methodology

The model package is composed of the phase-averaged spectral wave model WaveWatchIIITM, (Tolman 2008) here and after WW3, and of the Boussinesq-type nearshore wave model BOSZ developed by Roeber et al. (2010) and Roeber and Cheung (2012). WW3 solves the action balance equation using the latest physical parameterizations for the source terms (e.g. Ardhuin et al. 2010 and Filipot & Ardhuin, 2012). BOSZ is a NOAA approved model for inundation mapping and hazard mitigation. Recent efforts by Roeber et al. (2013) include the extension to higher order dispersion and nonlinearity ($kh \sim 7$) that allows calculation of wave transformation processes from fully deep water to shore. In this study, BOSZ uses wave spectra from WW3 as input and calculates wave-by-wave processes over the island shelf and in the surf zone including secondary effects such as infra-gravity wave motion and surf beat, thereby providing an accurate description of the high-velocity flows, runup, and inundation along the coastline.

The location of the wave spectra from WW3 is about 4 km southwest of Sein Island in 40 m water depth. The bathymetry and topography used for modelling the hydrodynamic conditions over the BOSZ domain comes from the Litto3D[®] program, conducted by IGN and SHOM, and includes high resolution LiDAR data as well as data from soundings.

3. Field campaign and site description

The field campaign PROTEVS VAGUES 2012 has been launched in September 2012 in the Iroise Sea. The Iroise Sea is fully exposed to storms generated in the North East Atlantic that often come with heavy winds, severe sea states, as well as storm surges. These components have been identified to significantly contribute to erosion along the shore line of the Iroise Sea (e.g., Suanes et al. , 2012). The typical tidal range along the shores of the investigation area is about 6 to 7 m with spring tidal currents locally reaching 3 to 4m/s. A number of instruments, including one Wamos radar device, five datawell wave buoys, five current profilers (Nortek aquapros and awacs), five seabird sbe26 tide gauges and nineteen ocean sensors (OSS) pressure gauges were deployed to measure the hydrodynamic conditions from the open sea up to the shoreline.

This work focuses on the modeling effort and the data gathered in the nearshore area around the Sein island and is restricted to the analysis of 5 instruments on February 11, 2013 (see Table 1 and Figure 1).

3.1 Sein Island

This iconic French island is located 7 km to the west of Pointe du Raz (westernmost point of France) and stretches over 3 km westward. Its western part is connected to the Chaussée de Sein, a shallow, narrow, and irregular shoal, known as an extremely hazardous place for mariners. Sein is hit by massive waves during wintertime that interact with strong tidal currents. Since most of the island lies only little above the peak astronomical tide level, which is 5.5 m above MSL, its inhabitants are threatened by storm surges and storm waves that frequently flood parts of the island, despite the ongoing efforts to protect the coastline with various coastal infrastructures. The 20 meters-wide isthmus that connects the populated east part of the island to the fresh water and electricity plant (located in the western part) is a critical point as it is exposed at either side to severe hydrodynamic forces with erosion potential. For these reasons two arrays of pressure gauges were installed on the north and south side of this isthmus. The northern beach is a typical pocket beach, with a steep slope covered with pebbles on the foreshore that extends to the sea through a rocky platform. It is exposed to NW swells, though likely sheltered by the offshore shallow and irregular rocky bathymetry. In

contrast, the southern beach consists of a wide flat rocky platform and it is fully open to SW swells that frequently approach the site during winter storms in Brittany.



Figure 1: Photography taken from a plane on February 11, 2013. One can clearly see Sein Island and its shoal extending westward.

Due to the irregular bathymetry and the exposure to rough ocean conditions, Sein island poses a very challenging environment for hydrodynamic numerical modeling.

4. Hydrodynamic observations around Sein Island

The present study focuses on the observations gathered over the south coast of Sein. Two offshore instruments were deployed: the buoy DW1 recorded the offshore incoming wave field and MAREE3 measured the water level out of the wave effects. In the nearshore AWAC1 recorded water levels, currents and waves at the edge of the surf zone and three pressure gauges were installed on the flat intertidal rocky platform of Korréjou cove (see Figure 2) and to observe waves and water levels. This deployment allows for analyses of the nonlinear wave transformation from offshore (DW1) to the coastline (OSSI10) as well the water level distortion induced by the hydrodynamic forces. Water levels were computed with the pressure recorded at MAREE2, AWAC1, OSSI10 to OSSI12 and the water density estimated with the formula of Fofonoff et al. (1983). The water temperature was recorded by MAREE3 and the salinity given by the pre-operational HYCOM simulations run for Previmer (www.previmer.org). The elevations of OSSI10 and OSSI12 above mean sea level were obtained by comparing their water levels to those of MAREE3 in calm conditions. The wave spectra

are derived from 30 min pressure bursts at 5Hz with a 2048 points FFT for the OSSI sensors and a 17min 4 sec wave record at 2 Hz and 256 points FFT in the AWAC1 case.

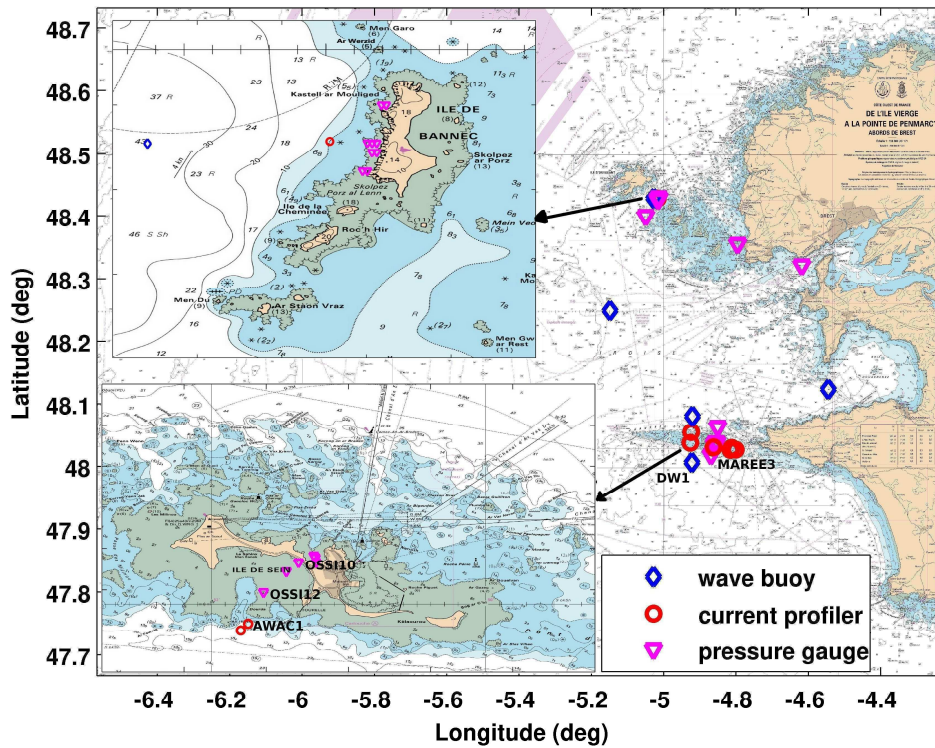


Figure 2: Site overview. Iroise Sea and Banneg and Sein islands (enclosed maps).

Instrument Name	Instrument Type	Measured quantity	Depth (m)
DW1	Datawell wave buoy	Directional wave spectra	45
MAREE3	Sea bird SBE26 tide gauge	Pressure	39
AWAC1	Nortek AWAC sensor	Pressure, current profile	14
OSSI12	Ocean sensor pressure gauge	Pressure	1
OSSI10	Ocean sensor pressure gauge	Pressure	-1

Table 1: instrument names, measured quantities and water depths with respect to MSL.

5. Numerical simulation

5.1. WaveWatchIII model setup

The model is run over an irregular grid, covering the Iroise Sea with a resolution ranging from a few kilometers offshore to about 200 meters near the coastline. The boundary conditions are provided by a 10' resolution model, nested in a global grid at 0.5° resolution. All models are forced with 1/8° 10

meters wind fields from the European Center for Medium-Range Weather Forecast. The Iroise Sea model takes currents and water levels into account that were produced by the HYCOM model operated by SHOM with a 1.7 km resolution.

This preliminary study focuses on the long swell event that hit Brittany on February 11, 2013. Offshore waves with peak significant wave heights of about 6 meters, peak period of 14 seconds and peak direction of 285° , propagated toward the coast bearing only light North West wind. A picture was taken from a plane flying over the area that day (Figure 1) where clean swell lines are refracting around the island and breaking over the shoal of Sein. This rather long swell conditions (only little affected by wind) is suitable to test case phase-resolving models such as the Boussinesq-type model BOSZ.

The model WW3 reproduces the wave conditions south of Sein with reasonable accuracy (See Figure 3). The selected wave event fell within a spring tide period with a tidal range of about 6 m and currents reaching 3 m/s. The effect of water levels and currents on the wave heights are clearly visible in Figure 3 and appears to be slightly underestimated by the model. Modeling of these effects has been investigated in details by Arduin et al. (2012) for the same geographical area. The good agreement with the observations at DW1 suggests that it is suitable to use WW3 spectra taken a few kilometers north of DW1 as boundary conditions for BOSZ. The use of wave spectra from a spectral model further demonstrates the versatility of this approach to assess the hydrodynamic conditions at remote sites. Often, no data is available to infer the offshore wave conditions, which makes it difficult to drive nearshore models with appropriate input. Spectral data from models like WW3 are relatively easy to obtain and can serve as appropriate input for phase-resolving wave models.

5.2. BOSZ model setup

The BOSZ domain includes the entire Sein island as well as a large portion of the open ocean to the West of it. The individual swell waves are generated along the western boundary by a source function added to the continuity equation. Even though the wavemaker function is able to generate the superposition of waves with different angles, it is advisable to align the offshore boundary with the peak swell direction to avoid unnecessary shadowing to either side of the domain. The WW3 wave spectrum at -4.89°W , 48.02°N in about 36 m water depth indicates a peak swell direction of 245° . Hence, the BOSZ domain is rotated by 25° anticlockwise. Sponge layers on all sides of the domain absorb the outgoing energy and act as open boundary condition. The domain is defined by a uniform Cartesian grid of 10.5 km length and 4.5 km width with 6m by 6m cells. To account for the local tidal elevation, the bathymetry was uniformly lowered by 2.5 m. The water depth at the location of the input wave spectrum from WW3 was then around 38 m, which consequently defines the offshore water depth in the domain near the wavemaker. The total runtime of BOSZ was 45 min to properly develop the offshore sea state and the nearshore wave setup. However, some of the low frequency infra-gravity modes would require an even longer computation. Though the nearshore dynamics are constantly affected by changes in tides, currents and wave energy, this study treats the wave spectrum discretely. In addition, the tide level is kept static over the entire model runtime. We therefore expect some discrepancies between model results and field data, especially in the high frequency band, since some of the wave-current interaction might not be resolved. Future studies regarding long-term nearshore dynamics will have to involve changes in the boundary conditions so that most of the dynamic system is accounted for.

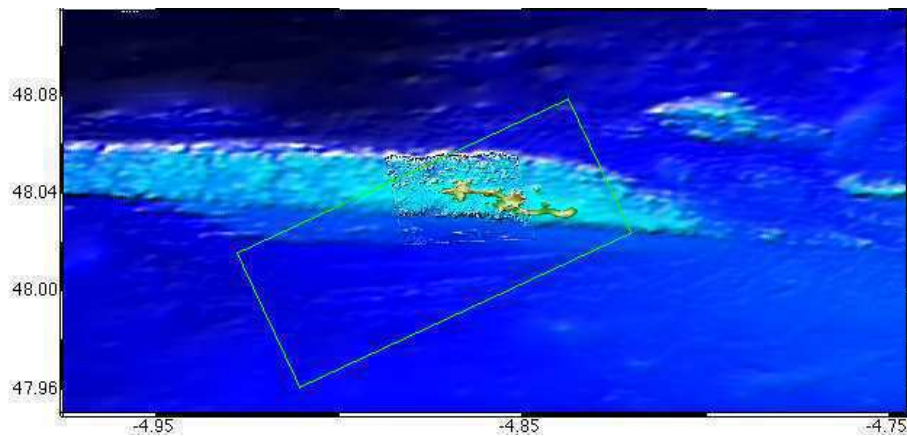
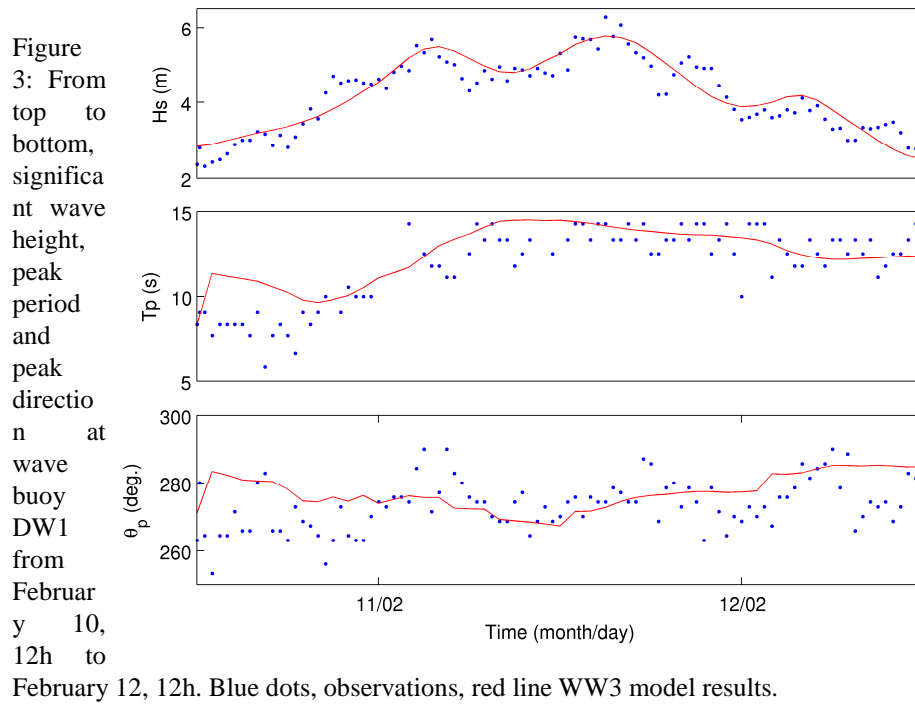


Figure 4: Bathymetry of Sein surroundings. The green tilted rectangle shows the BOSZ grid extension.

6. Results

On February 11 the significant wave height and peak period were almost constant at AWAC1 with mean values of 2.3 m and 13.9 s respectively. In contrast, the wave heights at OSS12 and OSS10 are fully driven by the water level as evident on Figure 5. Nearshore wave spectra recorded at AWAC1 OSS12 and OSS10 on February 11 2013 at 5 pm (high tide, water level about 2.5 m above MSL) are presented on Figure 6. They show strong spectral distortion across the rocky platform. At the AWAC1

location, the waves have undergone significant nonlinear transformation during the shoaling process as illustrated by the strong first peak harmonic at about 0.15 Hz. Wave breaking occurs shortly after. Past the break point, at OSSI12, the peak energy has been partly transferred toward the infra gravity band. Finally at the coastline (OSSI10), the spectrum significantly broadens and is dominated by the IG band. Note that the energy in this band is almost unchanged during the wave propagation between OSSI10 and OSSI12 (about 800 meters, or approximately 13 peak wavelengths). Indeed, most of the low frequency bound waves energy is relaxed as IG waves at the breaking point and it then propagates freely to the shore where it is dissipated or reflected.

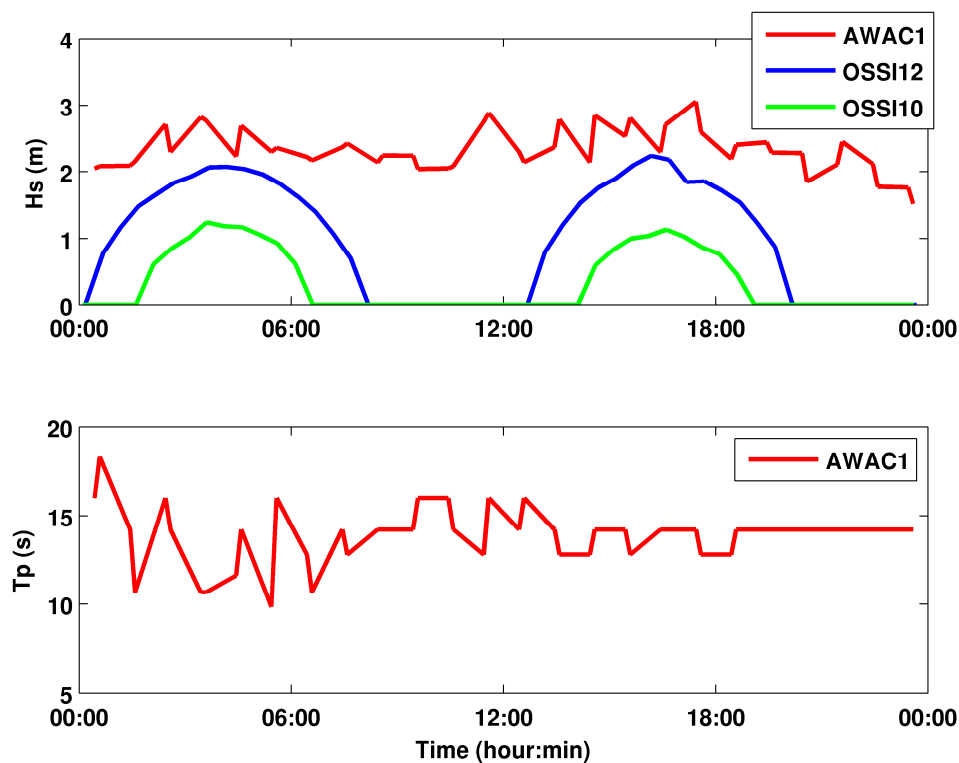


Figure 5: Significant wave height measured at AWAC1, OSSI12 and OSSI10 and peak period at AWAC1 on February 11, 2013.

This is indeed very similar to what was observed by Filipot and Cheung (2012) and Roeber and Cheung (2012) over a tropical coral reef (Mokuleia, Hawaii). A close look at the bathymetry indicates that Korréjou bottom is quite similar to the reef of Mokuleia, namely, consisting of a rather steep reef face, which is connected to the shore through a wide flat rocky/coral platform. The latter authors further reported that bottom friction dissipation commensurates with breaking dissipation in Mokuleia, a result already observed in coral reef environment by Lowe et al. (2007). These findings could probably apply to our study site, as visual observations suggest that only sparse wave breaking occurs over the rocky platform at high tide. Therefore, an important portion of the peak energy might get dissipated through bottom friction across the rough rocky platform at Korréjou cove. This would be confirmed by the fact that the IG energy band is roughly conserved between OSSI10 and OSSI12, advocating for light breaking between these two sensors. These questions will be investigated in the

near future.

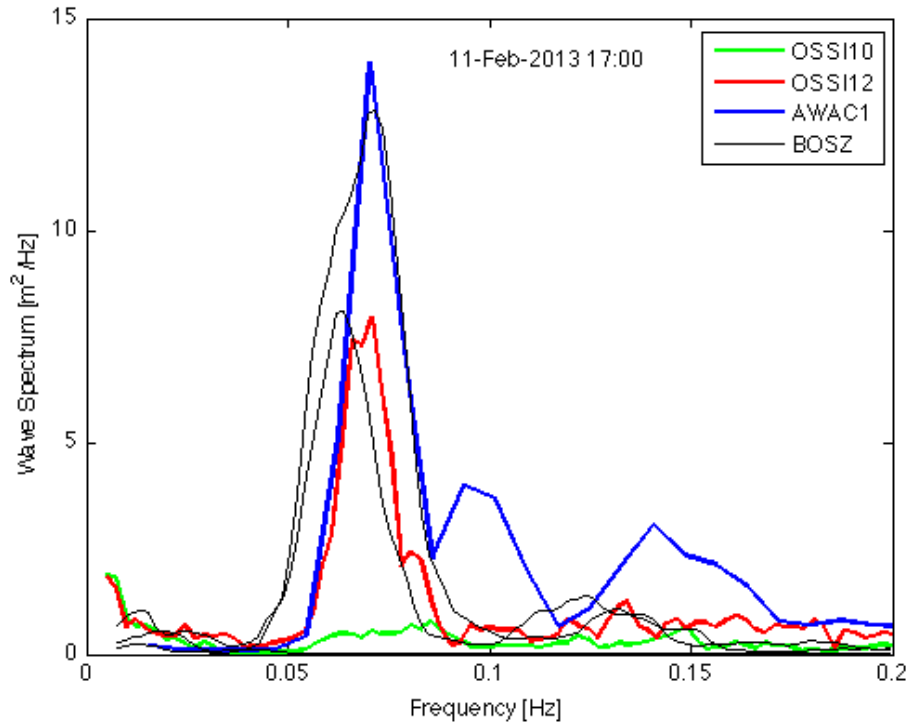


Figure 6: Wave spectra observed at AWAC1, OSSI12 and OSSI10 on February 11 2013 at 5pm. The black line shows the result of the BOSZ simulation.

The wave setup and surfbeat are among of the most hazardous phenomena of waves in the nearshore as they add up to the wave and pressure induced surge and increases the water levels. Once reflected by the shoreline, Infra gravity waves can be trapped nearshore by refraction and resonate as edge waves (e.g. Henderson et al., 2002). As mentioned before, Sein island is particularly vulnerable at its narrowest part, just where OSSI12 and 10 were deployed during the field campaign. The wave setup at these two locations was estimated for the considered wave event, by using MAREE3 as a reference for the still water level. As MAREE3 lies in 39 m depth and only little wind was blowing, it is a reasonable assumption. Interestingly, the wave setups observed at OSSI12 and OSS10 are not in phase. As the wave setup is induced by wave breaking at the entrance of the lagoon, about 800 m offshore of OSSI10, the setup at OSSI12 is probably influenced by an offshore shoal that may cause waves to break at low tide but not at high tide. Once the shoal is deep enough (at high tide), wave breaking stops and the wave setup at OSSI12 drops while it further increases at OSSI10 near the shoreline where it reached up to 35 cm in the morning (Figure 7). As waves focus and break on both sides of Korréjou cove entrance the water level patterns is complex and transient. Figure 8 shows the setup computed by BOSZ. With the main wave energy coming from west-southwest, more wave setup is observed at the eastern end of Korréjou Bay than in its center. Observations during the experiment confirm significant wave breaking at this location. BOSZ calculated a wave setup of 15 cm and 6 cm at OSSI12 and OSSI10 at 17:00 on February 11, 2013, which is in good agreement with the field observations.

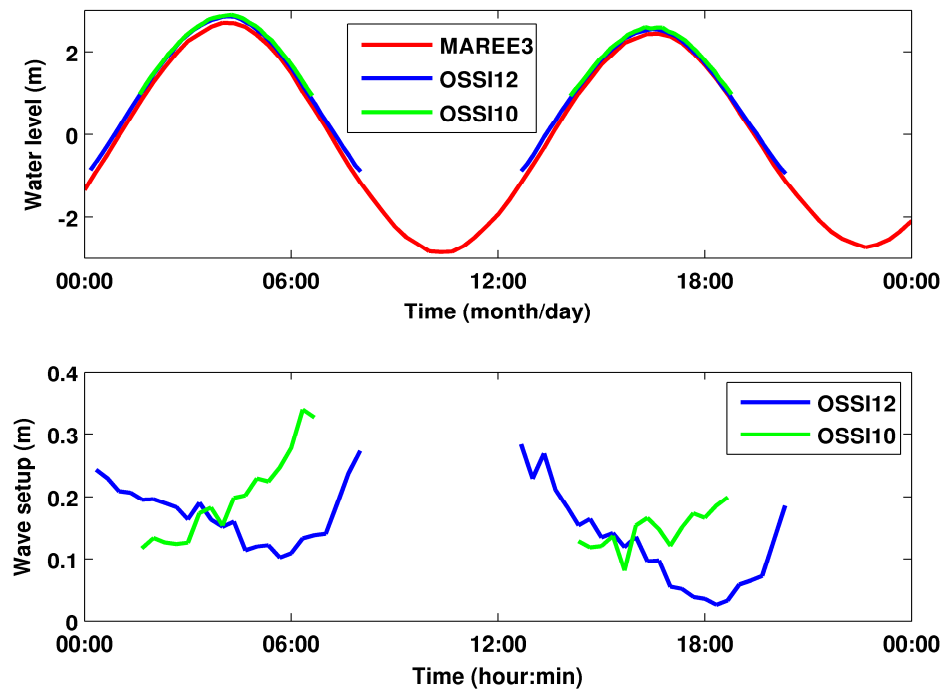


Figure 7: water levels and wave setup measured on February 11 at sensors MAREE2, OSSI12, OSSI10.

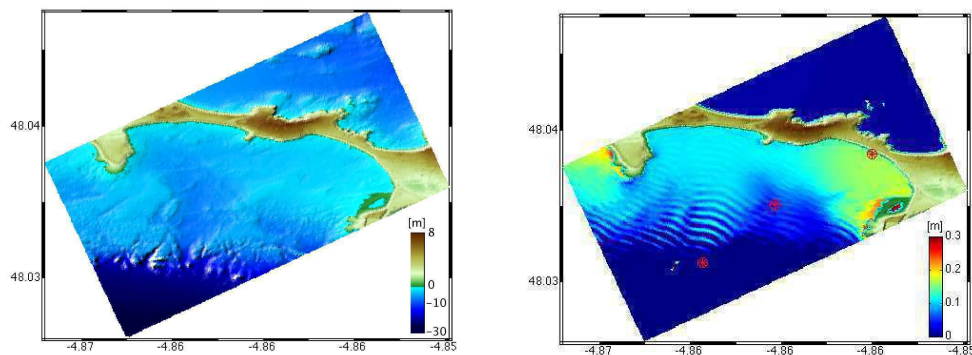


Figure 8: Bathymetry at high tide around 17:00 on February 11, 2013 (left). Wave setup from BOSZ at Korréjou Bay (right). Red circles denote sensor locations.

7. Conclusion

A sample of data from the PROTEVS VAGUES 2012 has been presented in this paper. Five sensors deployed South of Sein Island recorded a long swell event on February 11, 2013. They show strong nonlinear transformation of the wave field during its propagation to the shore. The nearshore spectra and water levels reveal, respectively a strong infra-gravity waves signal and wave setup respectively. Both processes can potentially be superimposed with wind and pressure induced effects, which may result in substantial surges in Korréjou cove that threaten the narrowest part of the islands. The

hydrodynamic processes reported in the present study are similar in many ways to those observed over coral reefs.

The spectral model, WW3, used to hindcast the waves in the coastal zone was found to accurately reproduce the conditions over the studied period. With the input wave spectrum from WW3, the Boussinesq-type wave model, BOSZ, not only captures the main hydrodynamic processes such as refraction, shoaling, and wave breaking, but also accounted for second-order processes such as wave setup and the inherent recirculation in the surf zone.

This study shows that the presented model approach can be effectively applied to challenging ocean conditions over highly irregular bathymetry.

Acknowledgements

We are grateful to the Parc Naturel Marin d'Iroise, the Réserve Naturelle d'Iroise for their assistance in preparing and accompanying the field experiment. We further thank the technical SHOM crew for their efforts in the realization of the campaign.

References

- Ardhuin, F., E. Rogers, A. Babanin, J.-F. Filipot, R. Magne, A. Roland, A. van der Westhuysen, P. Queffelec, J.-M. Lefevre, L. Aouf, and F. Collard, "Semi-empirical dissipation source functions for wind-wave models: part I, definition, calibration and validation," *J. of Phys. Oceanogr.*, 40 (9), 1917–1941.
- Ardhuin, F., Pineau-Guillou, L., Fichaut, F., Suanez, S., Corman D., Filipot J.-F. Extreme set-up and run-up on steep cliffs (Banneg Island, France), 2011. In proc. of the 12th International Workshop on Wave Hindcasting and Forecasting, Kohala Coast, Hawai'i, HI.
- Ardhuin, F., Roland, A., Dumas, F., Bennis, A. C., Sentchev, A., Forget, P., ... & Benoit, M. (2012). Numerical Wave Modeling in Conditions with Strong Currents: Dissipation, Refraction, and Relative Wind. *Journal of Physical Oceanography*, 42(12), 2101-2120.
- Booij N., Ris R.C., Holthuijsen L.H., 1999. A third-generation wave model for coastal regions, Part I, model description and validation. *J. Geophys. Res.*, 104(C4), 7649-7666.
- Fichaut, B. and Hallégouët B., 1989. Banneg une île dans la tempête. *Penn ar Bed*, 135, 36-43.
- Fichaut, B., Suanez, S., 2011. Quarrying, transport and deposition of cliff-top storm deposits during extreme events: Banneg Island, Brittany. *Marine Geology*, 238, 36-55.
- Filipot, J.-F. and Cheung, K.F., 2012. Spectral wave modeling in fringing reef environment. *Coastal Eng.*, 67(1), 67-79.
- Fofonoff, P. and Millard, R.C. Jr Unesco 1983. Algorithms for computation of fundamental properties of seawater, 1983. _Unesco Tech. Pap. in Mar. Sci., No. 44, 53 pp. Eqn.(15) p.18
- Henderson, S. M., & Bowen, A. J. (2002). Observations of surf beat forcing and dissipation. *Journal of Geophysical Research: Oceans (1978–2012)*, 107(C11), 14-1.
- Lowe, R. J., Falter, J. L., Bandet, M. D., Pawlak, G., Atkinson, M. J., Monismith, S. G., & Koseff, J. R. (2005). Spectral wave dissipation over a barrier reef. *Journal of Geophysical Research: Oceans (1978–2012)*, 110(C4).
- Roeber, V., Cheung, K.F., and Kobayashi, M.H., 2010. Shock-capturing Boussinesq-type model for nearshore wave processes. *Coastal Eng.*, 57(4), 407-423.
- Roeber, V., Cheung, K.F., 2012. Boussinesq-type model for energetic breaking waves in fringing reef environment. *Coastal Eng.*, 70(1), 1-20.
- Roeber, V., Heitmann, T., Cheung, K.F., 2013. A higher-order conservative Boussinesq-type model. In preparation.
- Suanez, S., Cariolet, J. M., Cancouët, R., Ardhuin, F., & Delacourt, C. (2012). Dune recovery after storm erosion on a high-energy beach: Vougot Beach, Brittany (France). *Geomorphology*, 139, 16-33.
- Tolman H.L. (2008). A mosaic approach to wind wave modeling. *Ocean Mod.*, 25(1), 35-47.